ISSN 1068-3755, Surface Engineering and Applied Electrochemistry, 2017, Vol. 53, No. 5, pp. 475–485. © Allerton Press, Inc., 2017.

Corrosion Inhibition and Adsorption Behavior of *Murraya koenigii* Extract for Corrosion Control of Aluminum in Hydrochloric Acid Medium[1]

Pushpanjali, Suma A. Rao, and Padmalatha Rao*

Department of Chemistry, Manipal Institute of Technology, Manipal University, Manipal-Karnataka, 576104 India

**e-mail: padmalatha.rao@manipal.edu*

Received August 15, 2016; in final form, December 2, 2016

Abstract—The corrosion behavior of aluminum in the hydrochloric acid medium of pH 3 was studied using Tafel polarization and electrochemical impedance spectroscopy techniques in the presence or the absence of the *Murraya koenigii* (commonly known as curry) leaves extract at 303 K to 323 K. The concentration of the inhibitor used was in a range of 0.05–0.4 gL^{-1}. The inhibition efficiency was found to increase with increasing the inhibitor concentration and decreasing temperature. Polarization data showed that the curry leaves extract (CLE) acted as anodic type of inhibitor at lower concentrations of the inhibitor and as mixed type at higher concentrations of the inhibitor. The maximal inhibition efficiency of 91.79% was obtained with the CLE at its optimum concentration of 0.4 gL^{-1}. Adsorption of the CLE was found to obey the Langmuir adsorption isotherm and underwent both physisorption and chemisorption process. The kinetic and thermodynamic parameters were calculated and discussed in detail. The results obtained by both methods were in good agreement with each other. The protective film formed on the surface of aluminum by the adsorption of inhibitor molecules present in the CLE in the hydrochloric acid medium of pH 3 was confirmed by the scanning electron microscopy and energy-dispersive X-ray spectroscopy. So, the CLE emerged as a potential, cost-effective and eco-friendly natural inhibitor for the corrosion control of aluminum in the hydrochloric acid medium.

Keywords: aluminum, green inhibitor, curry leaves, Tafel polarization, electrochemical impedance spectroscopy, scanning electron microscopy

DOI: 10.3103/S1068375517050088

INTRODUCTION

Aluminum is a valuable material due to its important properties: lightweight, strength, recyclability, corrosion resistance, durability, formability, and conductivity. Due to this unique combination of properties, the applications of aluminum continue to increase for industrial and domestic purposes. Good corrosion resistance of aluminum is due to its affinity for oxygen, this results in the formation of a very thin but tenacious oxide film that protects the surface from further oxidation. This oxide film is amphoteric and dissolves substantially when the metal is exposed to high concentrations of acids, bases, and salts [1].

Concentrated mineral acids such as hydrochloric acid are used extensively in pickling, industrial acid cleaning, cleaning of oil refinery equipment, acid descaling, chemical and electrochemical etching, and oil well acidizing of aluminum [2]. These contacts lead to the loss of the metal due to corrosion. A useful method to protect metals and alloys in aggressive environments is the addition of organic and inorganic inhibitors to the solution in contact with the surface so as to restrain the corrosion reaction and hence reduce the corrosion rate [3, 4]. A number of organic compounds are known to be appropriate corrosion inhibitors for aluminum in acidic environments [5]. Such compounds typically contain nitrogen, oxygen or sulfur in a conjugated system and function through the adsorption of the molecules on the metal surface, forming a barrier to a corrodent attack.

Though many synthetic organic compounds showed good anticorrosive activity, most of them are highly toxic to both human beings and the environment. The safety and environmental issues of corrosion inhibitors have always been a global concern. The toxicity may manifest either during the synthesis of a compound or during its applications [6].

Therefore, the usage of non-toxic and natural products as corrosion inhibitors have become important as they are environmentally friendly, biodegradable, readily availability, renewable sources that can be synthesized by a simple procedure with a low cost [7].

[1] The article is published in the original.

Table 1. Composition of material

Element	Si	Fe	Mg	Al
Composition, wt %	0.467	0.163	0.530	Balance

So far, lots of works have reported on using natural products as corrosion inhibitors [8, 9] for aluminum in an acidic medium.

We report herein the results of application of the Curry plant (*Murraya koenigii*), to be exact of the curry leaves extract (CLE) for the corrosion control of aluminum in the hydrochloric acid medium of pH 3. The CLE is composed of numerous organic heterocyclic compounds. Major constituents are reported to be Terpene 4-ol, Mahanimbine and β-elemene [10].

EXPERIMENTAL

Material

The experiments were performed with specimens of aluminum. The composition of the material used is given in Table 1. Cylindrical test coupons of 10 mm diameter and approximately of 20 mm height were machined from the rods of aluminum and metallographically mounted up to 10 mm height using cold setting resin. The exposed flat surface of the mounted part was polished as per standard metallographic practice–belt grinding followed by polishing on emery paper (in a range of 600–1200) and finally on a disc polishing wheel using the levigated alumina abrasive.

Preparation of Medium

The stock solution of 2 M hydrochloric acid was prepared by using the analar grade hydrochloric acid and double distilled water. Standardization was done by the volumetric method. From the standard solution, a hydrochloric acid solution of required concentrations was prepared as and when required. Experiments were carried out at five different temperatures using a calibrated thermostat under unstirred conditions.

Preparation and Characterization of Inhibitor and its Solution

The CLE was prepared by the method described elsewhere [10]. Curry leaves were cut into pieces. These were completely air-dried at room temperature for 4 weeks. The dried plant products were pulverized into a fine powder using a domestic mixer grinder. Next, 40 g of the powder was boiled in 500 mL of distilled water for 5 h. It was filtered using a piece of clean white cotton gauze. The filtrate was evaporated to complete dryness at 40°C, producing a fine sweet smelling and of the chocolate color solid residue. The extraction process was repeated 4–5 times and the solid residue weighed after extraction was pooled together and ground into a fine powder using mortar. The CLE was then stored in an air and water-proof container and kept in a refrigerator at 4°C. An aqueous solution of the inhibitor of required concentrations was prepared freshly as and when required.

Spectral Studies of Aqueous Plant Extract

The Fourier transform infrared spectrum of the dried sample was recorded using a spectrophotometer in a frequency range of 4000 to 400 cm^{-1}, with the KBr pellet technique.

Electrochemical Measurements

Electrochemical studies were carried out using an electrochemical workstation with a conventional three electrode Pyrex glass cell with platinum as a counter electrode and SCE as a reference electrode. The working electrode was aluminum. Finely polished aluminum specimen was exposed to 50 mL hydrochloric acids of pH 3 at different temperatures (30 to 50°C), which allowed to establish a steady state open circuit potential by immersing the electrodes in the corrosive medium for 1800 s. Experiments were performed by placing the cell in a calibrated thermostat, under unstirred conditions.

Potentiodynamic Polarization Measurements

The potentiodynamic current potential plots were recorded by polarizing the specimens from –250 mV cathodically to +250 mV anodically with respect to the open circuit potential at a scan rate of 1 mV s^{-1}. The experiments were carried out in the presence or the absence of different concentrations of the inhibitor.

Electrochemical Impedance Spectroscopy Studies

In the electrochemical impedance spectroscopy (EIS), an AC signal of a small amplitude, of 10 mV and a frequency spectrum from 100 kHz to 0.01 Hz was impressed at the open circuit potential. The EIS analysis was carried out immediately after the potentiodynamic polarization (PDP) without further surface treatment. In both measurements, a minimum of 3–4 trials was done and the average of best three agreeing values was reported.

Scanning Electron Microscopy and Energy–Dispersive X-ray Spectroscopy

The morphology of the aluminum surface, in the presence or the absence of the inhibitor, was studied by immersing the material in a hydrochloric acid medium of pH 3 for 2 h using an analytical scanning electron microscope. The energy-dispersive X-ray (EDX) analysis was carried out to study the elemental

mapping for the same sample after taking the scanning electron microscopy (SEM) images.

RESULTS AND DISCUSSIONS

Potentiodynamic Polarization Method

Valuable potentiodynamic polarization parameters like the corrosion current density (i_{corr}), the corrosion potential (E_{corr}), the anodic Tafel slope (β_a) and the cathodic Tafel slope ($-\beta_c$) were obtained from the PDP plots in Fig. 1.

The corrosion rate was calculated using Eq. (1) [11]:

$$\text{C.R.}\left(\text{mm Y}^{-1}\right) = \frac{i_{corr} M \times 3270}{\rho Z}, \quad (1)$$

where 3270 is a constant that defines the unit of the corrosion rate, i_{corr} is the corrosion current density in A cm^{-2}, ρ is the density of the corroding material (g cm^{-3}), M is the atomic mass of the metal, and Z is a number of electrons transferred per a metal atom. For aluminum, $Z = 27$ and $\rho = 2.7$ g cm^{-3}.

The percentage of the inhibition efficiency was calculated using equations (2) and (3):

$$\text{I.E. } (\%) = \theta \times 100, \quad (2)$$

where

$$\theta = \frac{i_{corr} - i_{corr\,(inh)}}{i_{corr}}, \quad (3)$$

where i_{corr} and $i_{corr(inh)}$ are the corrosion current densities in the absence and in the presence of the inhibitor, respectively. From the corrosion potential (E_{corr}) the corrosion current density (i_{corr}), the corrosion rate (C.R.) and the percentage of the inhibition efficiency (% I.E.) were calculated.

With an increase in concentrations of the CLE, the corrosion current density decreased. The inhibition efficiency increased with increasing inhibitor concentrations. The observed inhibition efficiency of the CLE may be due to the adsorption of its components on the aluminum surface. The adsorbed molecules may isolate the metal surface from the aggressive medium leading to a decrease in the corrosion rate [7].

The anodic polarization curves did not exhibit any linear behavior and are assumed to represent anodic oxidation of aluminum. The anodic branches showed the inflection points at potentials more positive than the corrosion potential (E_{corr}), characterized by two different slopes indicating a kinetic barrier effect, possibly due to the deposition of a surface film followed by its dissolution at an increased anodic potential [11]. However, the cathodic branch of polarization curves showed the linear behavior and is thought to represent the cathodic hydrogen evolution through the reduction of water. The cathodic Tafel slopes remained almost unchanged for both uninhibited and inhibited

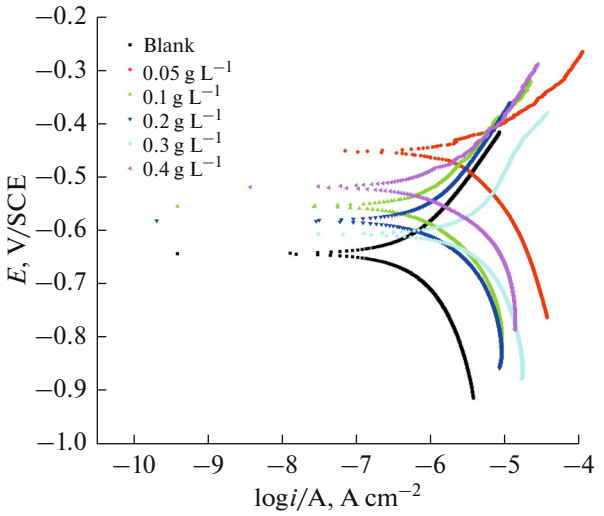

Fig. 1. PDP plots for corrosion of aluminum with different concentrations of CLE in HCl of pH 3 at 30°C.

solutions. This indicated that the inhibitive action of the CLE may be due to simple blocking of the available surface area on the metal surface. In other words, the inhibitor diminishes the surface area available for hydrogen evolution without affecting the reaction mechanism, only causing inactivation of a part of the surface [12, 13].

There was a measurable positive shift (in a range of 86 to 250 mV) in the corrosion potential (E_{corr}) after the addition of the inhibitor (0.05–0.2 gL^{-1}) at lower concentrations. According to reported literature [14], if the displacement in the corrosion potential after the addition of the inhibitor is more than ±85 mV with respect to the corrosion potential of the uninhibited solution, then the inhibitor can be considered distinctively as either a cathodic or anodic type. In the present investigations, for the hydrochloric acid medium of pH 3 for lower concentrations (0.05–0.2 gL^{-1}) of the inhibitor, a shift in the corrosion potential was towards the positive direction and it was more than 85 mV. This observation suggested that constituents of the inhibitor molecule may act as an anodic type inhibitor and bring the anodic reaction under control. But at higher concentrations of the inhibitor, the shift in the corrosion potential was less than ±85 mV (in a range of 1–80 mV), with the potential slightly shifted towards a positive direction. This observation suggested that constituents of the inhibitor molecule act as the mixed type and control both anodic and cathodic reactions, preferentially bringing down the anodic reaction, under control.

Electrochemical Impedance Spectroscopy

Figure 2 represent the Nyquist plot for the corrosion of aluminum in hydrochloric acid, pH 3, with dif-

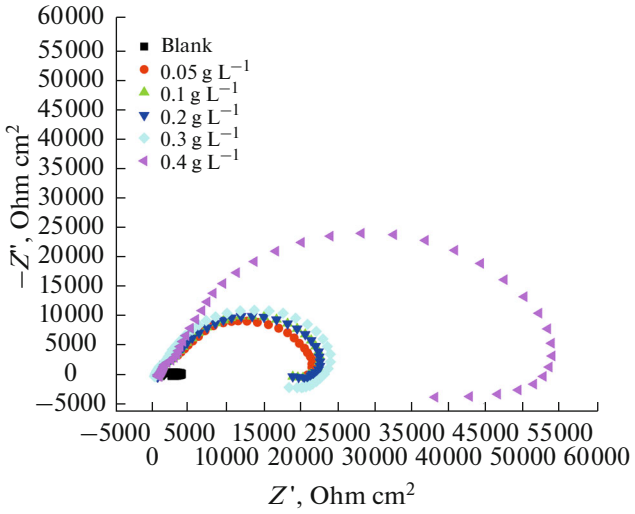

Fig. 2. Nyquist plot for aluminum corrosion in HCl of pH 3, with different concentrations of CLE, at 30°C.

ferent concentrations of the CLE at 30°C. Similar plots were obtained under other studied temperatures.

The impedance plots are semicircles. The plot in Fig. 2 indicates that the corrosion process is mainly charge transfer controlled. The presence of the inhibitor raised the impedance but did not change the mechanism of corrosion. It is in accordance with the observations obtained from the polarization measurements that demonstrated that the inhibitor does not alter the mechanism of electrochemical reactions responsible for corrosion. It inhibits corrosion primarily through adsorption of the inhibitor on the metal surface [15]. The impedance plots are with a depressed capacitive loop at a high-frequency range followed by an inductive loop at a low-frequency region. Similar impedance plots have been reported in literature for the corrosion of pure aluminum and aluminum alloys in various electrolytes [16].

The high-frequency capacitive loop could be assigned to the charge transfer of the corrosion process and to the formation of an oxide layer. The oxide film is considered to be a parallel circuit of a resistor due to the ionic conduction in the oxide film and a capacitor due to its dielectric properties. According to the reported literature [16], the capacitive loop is corresponding to the interfacial reactions, particularly, to the reaction of aluminum oxidation at the metal/oxide/electrolyte interface. The process includes the formation of Al^+ ions at the metal/oxide interface and their migration through the oxide/solution interface where they are oxidized to Al^{3+}. At the oxide/solution interface, OH^- or O^{2-} ions are also formed. The fact that all these three processes are represented by only one loop could be attributed either to the overlapping of the loops of processes or to the assumption that one process dominates and, therefore, excludes all other processes. Another explanation of a high-frequency capacitive loop is the oxide film itself. This was supported by a linear relationship between the inverse of the capacitance and the potential [14, 17]. The origin of the inductive loop has often been attributed to the surface or bulk relaxation of species in the oxide layer [15]. The low frequency inductive loop may be related to the relaxation process obtained by adsorption and incorporation of the sulfate ions, oxide ion and charged intermediates on and into the oxide film. As the inhibitor concentrations increased, the diameter of the inductive loop went on decreasing, which may be due to the increase in the adsorption of the inhibitor indicating a decrease in the relaxation process. At a higher concentration of the inhibitor, the inductive loop disappears, which may be because the adsorption of inhibitor molecules reduces the metal dissolution at the metal-solution interface.

As shown in Fig. 2, the obtained semicircles were depressed in the absence or in the presence of the inhibitor. A deviation of this kind is referred to as frequency dispersion. It has been attributed to inhomogeneities of solid surfaces. It was suggested elsewhere [13] that an exponent "n" in the impedance function can be considered a deviation parameter from the ideal behavior. By this suggestion, the capacitor in the equivalent circuit can be replaced by a so-called constant phase element that is a frequency-dependent element related to the surface roughness [15].

The impedance function of the constant phase element (CPE) has following form:

$$Z_{CPE} = 1/(Y_0/\omega)^n, \quad (4)$$

where the amplitude Y_0 and n are frequency independent, and ω is the angular frequency for which—Z'' reaches its maximum, n is dependent on the surface morphology, with values $-1 \le n \le 1$. Y_0, and n can be calculated by the equations as in [11].

An equivalent circuit consisting of nine elements, for the interpretation of the measured impedance data of the aluminum in hydrochloric acid medium is shown in Figs. 3a, 3b.

In these equivalent circuits, R_s is the solution resistance and R_t is the charge transfer resistance. R_L and L represent the inductive elements. The CPE (Q) is in parallel to the series capacitors C_1, C_2 and series resistors R_1, R_2, R_L and R_t. R_L is in parallel with the inductor L.

The double layer capacitance (C_{dl}) was calculated via equation (5):

$$C_{dl} = C_1 + C_2. \quad (5)$$

The polarization resistance (R_p) was calculated via equation (6):

$$R_p = R_L + R_t + R_1 + R_2. \quad (6)$$

Since the polarization resistance (R_p) is inversely proportional to the corrosion current, it can be used to

calculate the percentage of the inhibition efficiency (% I.E.) using relation (7):

$$\text{I.E.}\% = \frac{R_{p(inh)} - R_p}{R_{p(inh)}} \times 100, \quad (7)$$

where $R_{p(inh)}$ and R_p are the polarization resistances in the presence or the absence of the inhibitor.

As seen from Fig. 2, the solution resistance (R_s) remained almost constant, with and without the addition of the CLE for aluminum. It was also observed that the value of the CPE (Q) decreased, while the values of the charge transfer resistance (R_t) increased with a higher concentration of the inhibitor. This observation indicates that the inhibition efficiency increases with an increase in the concentration of the CLE.

The double layer between the charged metal surface and the solution is considered to be an electrical capacitor. The adsorption of the inhibitor molecules on the aluminum surface diminishes its electrical capacity because there arrears the displacement of the water molecules and other ions originally adsorbed on the surface. The decrease in this capacity with an increase in the inhibitor concentrations may be attributed to the formation of a protective layer on the electrode surface. The thickness of this protective layer increased with increase in inhibitor concentration up to their critical concentration of 0.4 gL^{-1} and then decreased. The obtained CPE (Q) values decreased noticeably with an increase in the concentrations of inhibitor. This may be due to the adsorption of constituents of CLE on the metal surface as Q is inversely proportional to the thickness of the protective layer [15].

The measured values of polarization resistance was found to increase with the increasing concentrations of CLE. It may be due to the decrease in the corrosion rate for the aluminum with an increase in inhibitor concentration. This is in accordance with the observations obtained from potentiodynamic measurements. Results of the PDP and EIS are in Table 2.

Effect of Temperature

Inhibition efficiency of the CLE decreased with increase in temperature. This can be attributed to the decrease in the protective nature of the inhibitive film formed on the metal surface (or desorption of the inhibitor molecules on the metal surface) at higher temperatures [11]. This suggests physical adsorption mechanism. Physical (electrostatic) adsorption may take place when inhibition efficiency decreases with increase in temperature (whereas chemical adsorption takes place when inhibition efficiency increases with increase in temperature) [11–13]. However, at higher concentrations of inhibitor, this decrease was small. The study of the effect of temperature was used to calculate the energy of activation (E_a) for the corrosion

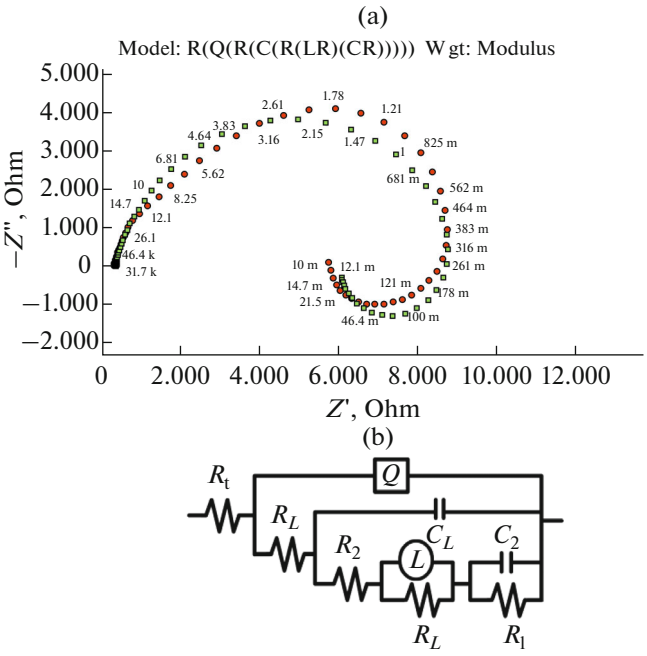

Fig. 3. (a) EIS data for aluminum corrosion in HCl of pH 3 containing CLE (0.4 gL^{-1}) at 30°C interpreted by equivalent circuit; (b) Equivalent circuit.

process in the presence or the absence of inhibitor using Arrhenius rate law Equation (8) [11].

$$\ln \text{CR} = B - \frac{E_a}{RT}, \quad (8)$$

where B is a constant which depends on the metal type and R is the universal gas constant (R = 8.314 $Jmol^{-1}K^{-1}$), T is the absolute temperature. Plots of ln(CR) versus $1/T$ gave straight lines with a slope (slope = $-E_a/R$). The Arrhenius plot for the corrosion of aluminum in the hydrochloric acid medium of pH 3 in the absence and in the presence of inhibitor is shown in Fig. 4. The values of enthalpy of activation (ΔH_a) and entropy of activation (ΔS_a) for corrosion and inhibition process were calculated from transition state equation (9) [11].

$$\text{CR} = \left(\frac{RT}{Nh}\right)\exp\left(\frac{\Delta S_a}{R}\right)\exp\left(-\frac{\Delta H_a}{RT}\right), \quad (9)$$

where h is Plank's constant ($h = 6.626 \times 10^{-34}$ Js) and N is Avogadro's number ($N = 6.023 \times 10^{23}$).

The plot of ln (CR/T) vs $1/T$ for the corrosion of aluminum in hydrochloric acid containing different concentrations of the CLE is shown in Fig. 5. Plot of ln (CR/T) vs $1/T$ gave straight lines with a slope = $-\Delta H_a/R$, and an intercept = $\ln R/Nh + \Delta S_a/R$. Results are tabulated in Table 3.

As is clear from Table 3, the energy of activation (E_a) increased significantly after the addition of the inhibitor. The increase in the activation energy (E_a) of

Table 2. Results of PDP and EIS measurements for corrosion of aluminum in hydrochloric acid, pH 3, with different concentrations of CLE, at different temperatures

		PDP				EIS		
Temp., K	CLE, gL^{-1}	i_{corr}, $\mu A\ cm^{-2}$	$-\beta_c$, $mV\ dec^{-1}$	E_{corr}, mV vs SCE	% I.E.	C_{dl}, $\times 10^{-10}$ $F\ cm^{-2}$	R_p, Ohm cm^2	% I.E.
303	0.0	7.05	603	−654	–	32.9	6068	–
	0.05	2.06	632	−466	70.82	10.6	23878	74.58
	0.1	1.20	661	−555	82.97	6.7	26653	78.23
	0.2	0.96	586	−582	86.34	3.1	27484	79.91
	0.3	0.81	496	−644	88.55	2.3	32127	81.11
	0.4	0.58	719	−619	91.79	0.9	49664	87.78
308	0.0	7.49	644	−659	–	111.0	6036	–
	0.05	2.31	629	−453	69.02	11.0	22878	73.62
	0.1	2.11	642	−473	71.79	7.6	23373	74.17
	0.2	1.89	641	−521	74.74	5.7	24474	75.34
	0.3	1.09	725	−604	85.49	5.2	31147	80.62
	0.4	0.81	741	−624	89.23	3.9	32684	81.53
313	0.0	7.97	651	−556	–	158.0	6013	–
	0.05	3.68	632	−461	53.81	25.4	18665	67.78
	0.1	2.51	533	−479	68.49	15.8	21065	71.45
	0.2	2.12	641	−498	73.37	7.9	22262	72.99
	0.3	1.71	658	−548	78.47	4.1	29184	79.39
	0.4	0.88	748	−495	88.01	3.7	30949	80.57
318	0.0	9.22	615	−633	–	461.0	4550	–
	0.05	4.53	610	−449	50.83	24.1	13878	49.97
	0.1	3.32	587	−473	63.98	10.4	14779	69.20
	0.2	2.54	680	−537	72.44	9.1	15255	70.17
	0.3	2.13	678	−543	76.87	4.0	20295	77.57
	0.4	1.09	747	−593	87.12	3.1	21763	79.08
323	0.0	9.33	505	−665	–	552.0	4363	–
	0.05	5.33	453	−480	42.94	74.2	8320	47.55
	0.1	4.38	566	−484	53.06	36.1	9778	55.37
	0.2	3.22	513	−482	65.46	8.9	13884	68.57
	0.3	2.31	596	−642	75.20	7.7	18971	76.99
	0.4	1.20	663	−648	86.08	3.3	20166	78.36

inhibited solutions compared to that of the blank suggests that the inhibitor gets adsorbed on the corroding metal surface. An increase in the energy of activation (E_a), at higher inhibitor concentrations indicate the increase in the energy barrier for the corrosion reaction [13]. The adsorption of the inhibitor molecules on the aluminum surface blocks the charge transfer during corrosion reaction, thereby increasing the activation energy. In other words, the adsorption of the inhibitor on the electrode surface leads to the formation of a physical barrier that reduces the metal reactivity in the electrochemical reactions of corrosion [12].

The enthalpy of activation (ΔH_a), as the energy of activation, was higher in the presence of the inhibitor than in its absence, and it was positive. The former may be due to the adsorption of the inhibitor molecules on the metal surface and the latter may be due to the endothermic nature of the aluminum dissolution in hydrochloric acid [11].

The inhibition efficiency decreased with an increase in temperature which may be due to the desorption of the inhibitor molecules with an increase in temperature [12]. The values of the entropy of acti-

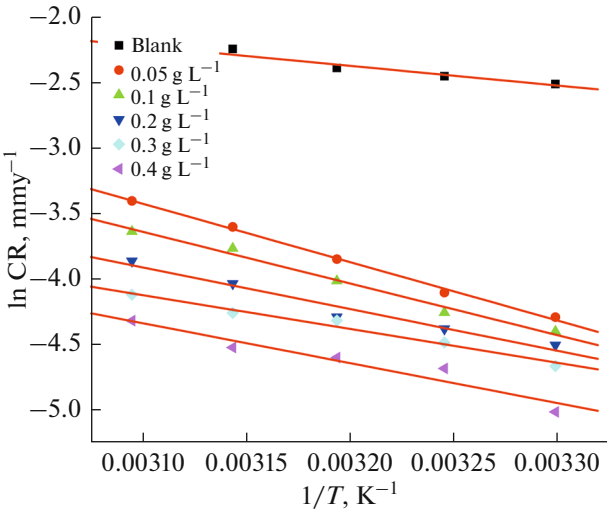

Fig. 4. Arrhenius plot for the corrosion of aluminum containing different concentrations of CLE in HCl of pH 3.

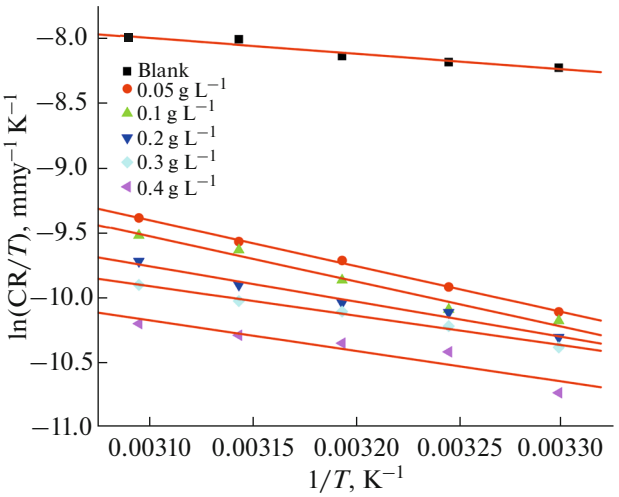

Fig. 5. Plot of ln(CR/T) vs $1/T$ for corrosion of aluminum in HCl, pH 3, with different concentrations of CLE.

vation (ΔS_a) were higher for inhibited solutions than those for the uninhibited ones. This suggested that a decrease in randomness occurred ongoing from reactants to the activated complex. This might be the result of the adsorption of organic compounds present in the CLE from the acidic solution, which could be regarded to be a quasi-substitution process between the organic compounds in the aqueous phase and water molecules at the electrode surface. In this situation, the adsorption of the inhibitor is accompanied by the desorption of water molecules from the surface. Thus the increase in the entropy of activation (ΔS_a) was attributed to an increase in the solvent entropy [11–13].

Adsorption Considerations

Inhibitors are known to decrease metal dissolution via adsorption on the metal/corrodent interface to form a protective film that separates the metal surface from the corrosive medium. The adsorption route is usually regarded as a substitution process between the inhibitor in the aqueous solution [$Inh_{(sol)}$] and water molecules adsorbed at the metal surface [$H_2O_{(ads)}$] as given in reaction (10) borrowed from [13]:

$$Inh_{(sol)} + nH_2O_{(ads)} \leftrightarrow Inh_{(ads)} + nH_2O_{(sol)}, \quad (10)$$

where n is a number of water molecules replaced by one molecule of the adsorbed inhibitor. The adsorption bond strength is dependent on the composition of the metal, corrodent, inhibitor structure, concentration and orientation as well as on temperature. Adsorption isotherms are usually employed to explain the mechanism of interaction between an inhibitor (adsorbate) and an adsorbent surface. This is achieved by fitting the degree of the surface coverage data into various adsorption isotherms or models; the correlation coefficient (highest) is used to determine the best fit isotherm which can then be used to describe the inhibitor adsorption mechanism. In this work, the best-fit isotherm was the Langmuir adsorption model which relates the degree of the surface coverage (θ) to the concentration of the extracts (C_{inh}) according to equation (11):

$$\frac{\theta}{1-\theta} = K_{ads}C, \quad (11)$$

where K_{ads} is the equilibrium constant of the inhibitor adsorption process, C is the inhibitor concentration, and θ is the degree of the surface coverage, which was calculated using equation (3). This model has also been used for other inhibitor systems [18]. With hydrochloric acid, plots of C_{inh}/θ vs C_{inh} gave straight lines with an intercept = $1/K$). The Langmuir adsorption isotherms are shown in Fig. 6.

The correlation coefficient (R^2) was used to choose the isotherm that best fit the experimental data. The linear regression coefficients were close to unity and the slopes of straight lines were near unity, which sug-

Table 3. Activation parameters for corrosion of aluminum in hydrochloric acid, at pH 3, with different concentrations of CLE

CLE, gL^{-1}	E_a, $kJmol^{-1}$	ΔH_a, $kJmol^{-1}$	ΔS_a, $kJmol^{-1}K^{-1}$
0.0	12.49	9.89	−161.69
0.05	77.48	74.88	−234.78
0.1	67.16	64.55	−324.96
0.2	32.82	30.21	−211.64
0.3	16.51	13.91	−158.25
0.4	22.09	19.49	−173.42

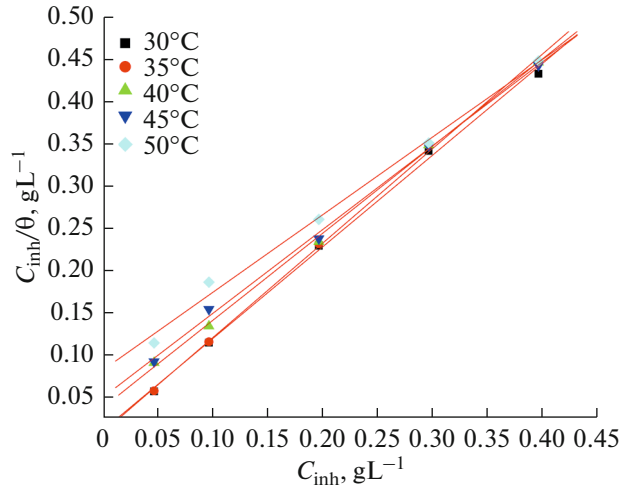

Fig. 6. Langmuir adsorption isotherms for adsorption of CLE on aluminum in HCl, pH 3.

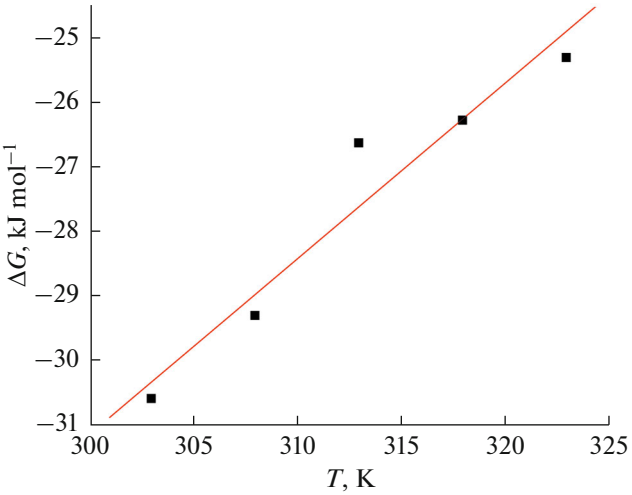

Fig. 7. Plot of ΔG°_{ads} vs T for adsorption of CLE on aluminum in HCl, pH 3.

gested that the adsorption of organic compounds present in the CLE obeyed the Langmuir adsorption isotherm and there was a negligible interaction between the adsorbed molecules [18].

Table 4. Thermodynamic parameters for adsorption of CLE on aluminum in hydrochloric acid, pH 3

Temp., K	ΔG°_{ads}, kJmol^{-1}	ΔH°_{ads}, kJmol^{-1}	ΔS°_{ads}, kJmol^{-1}K^{-1}
303	−30.56		
308	−29.28		
313	−26.61	−112.50	−0.271
318	−26.26		
323	−25.29		

Adsorption/desorption constant (K) is related to the standard free energy of adsorption (ΔG°_{ads}) by relation (12):

$$K = \frac{1}{C_{water}} \exp\left[\frac{\Delta G^{\circ}_{ads}}{RT}\right], \quad (12)$$

where C_{water} is the concentration of water in the solution expressed in gL^{-1}, R is the universal gas constant (8.314 Jmol^{-1}K^{-1}) and T is the absolute temperature. It must be noted that the concentration unit of water molecules has to be same as that of the inhibitor (the unit of C_{water} is gL^{-1} with the value of approximate 1×10^3). The calculated free energy of adsorption (ΔG°_{ads}) values (at different temperatures) obtained for hydrochloric acid medium of pH 3 are listed in Table 4 [18].

Negative values of the free energy of adsorption (ΔG°_{ads}) suggest the spontaneous adsorption of the inhibitor on the surface of the metal and the stability of the adsorbed layer on aluminum. The plot of ΔG°_{ads} vs T was used to calculate the standard enthalpy of adsorption (ΔH°_{ads}) and the standard entropy of (ΔS°_{ads}) according to the thermodynamic equation (13):

$$\Delta G^{\circ}_{ads} = \Delta H^{\circ}_{ads} - T\Delta S^{\circ}_{ads}. \quad (13)$$

The plot of ΔG°_{ads} vs T for aluminum in the hydrochloric acid medium of pH 3 is shown in Fig. 7.

Figure 7 clearly shows the dependence of ΔG°_{ads} on T, which indicates good correlation among thermodynamic parameters presented in Table 4.

The values of the standard free energy of adsorption (ΔG°_{ads}) for the adsorption of the CLE on the aluminum surface in studied concentrations of hydrochloric acid medium of pH 3 were more than −20 kJ mol^{-1} and less than −40 kJmol^{-1}, which indicates that the adsorption of constituents of the CLE on the surface of aluminum is a mixture of chemisorption and pysisorption [11].

In general, the standard free energy of adsorption (ΔG°_{ads}) values of adsorption of −20 kJmol^{-1} or less negative are associated with an electrostatic interaction between the charged molecules and the charged metal surface, resulting in physisorption. The standard free energy of adsorption (ΔG°_{ads}) values of −40 kJmol^{-1} or more negative involve charge sharing or transfer from the inhibitor molecules to the metal surface to form a coordinate covalent bond, resulting in chemisorption [18].

While an endothermic adsorption process ($\Delta H^{\circ}_{ads} > 0$) is attributed unequivocally to chemisorption, an exothermic adsorption process ($\Delta H^{\circ}_{ads} < 0$)

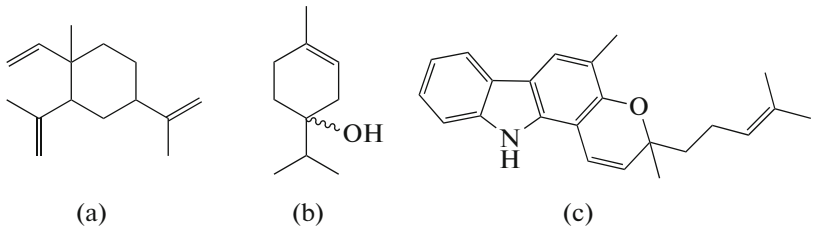

Fig. 8. (a) Structure of β-elemene; (b) Structure of Terpene 4-ol; (c) Structure of Mahanimbine.

may involve either physisorption or chemisorption or a mixture of both processes. In an exothermic process, physisorption is distinguished from chemisorption by considering the absolute value of adsorption enthalpy. According to the reported literature, for physisorption process enthalpy of adsorption is lower than 41.86 kJmol^{-1}, and for chemisorption process, the value approaches 100 kJmol^{-1} [18].

In the present investigation with the CLE as inhibitor, the calculated value of the enthalpy of adsorption (ΔH°_{ads}) is −112.50 kJ mol^{-1} in the hydrochloric acid medium of pH 3. This suggests that the adsorption of the CLE on the surface of aluminum is a mixture of both processes. The value of enthalpy of adsorption (ΔH°_{ads}) is nearer −100 kJmol^{-1}, which indicates that the extent of chemisorption is higher when compared to physisorption. The entropy of adsorption (ΔS°_{ads}) value is negative, indicating that an ordering takes place when the inhibitor gets adsorbed on the metal surface.

Mechanism of Corrosion and Inhibition Process

The CLE is composed of numerous natural organic heterocyclic compounds. Major constituents of the aqueous CLE are reported to be β-elemene, Terpene 4-ol, and Mahanimbine. Their structures are given in Figs. 8a–8c, respectively.

The presence of these compounds is confirmed by taking the IR spectrum of the CLE. Figure 9 shows the FTIR spectrum of aqueous extracts of the CLE. Absorption at 3425.34 cm^{-1} can be assigned to the stretching frequency of O–H. The peak at 2931 cm^{-1} can be assigned to the stretching mode of C–H group of alkanes. The 1404.04 cm^{-1} band is assigned to the C–H bending. The adsorption band at 1596 cm^{-1} is assigned to the C=C stretch of alkenes.

The surface of aluminum is covered with a thin layer of γ alumina which initially thickens on exposure to a neutral aqueous solution, with the formation of a layer of crystalline hydrated alumina. The aluminum surface has a positive charge when in an acidic environment. The mechanism of adsorption can be predicted on the base of the mechanism proposed for the corrosion of aluminum in hydrochloric acid [19].

Anodic reactions

$$Al_{(s)} + H_2O \leftrightarrow AlOH_{ads} + H^+ + e^-; \quad (14)$$

$$AlOH_{ads} + 5H_2O + H^+ \leftrightarrow Al^{3+}6H_2O + 2e^-; \quad (15)$$

$$Al^{3+} + H_2O \leftrightarrow [AlOH]^{2+} + H^+; \quad (16)$$

$$[AlOH]^{2+} + X^- \leftrightarrow [AlOHX]^+. \quad (17)$$

Cathodic reactions

$$H^+ + e^- \rightarrow H(ads); \quad (18)$$

$$H(ads) + H(ads) \rightarrow H_2. \quad (19)$$

Two modes of the adsorption process could be suggested to explain the inhibitory action of the CLE for the corrosion of aluminum in hydrochloric acid medium. In aqueous acidic solutions, Mahanimbine, Terphene 4-ol and β-elemene molecules may exist either as unprotonated molecule or in the form of protonated species [20].

The CLE acts as an anodic type at lower concentrations of the inhibitor and brings down anodic reactions under control. In an acid medium, aluminum is positively charged since the pH of the potential of zero charges for aluminum at the oxide/solution interface is 9.0–9.1. This will attract negative chloride ions from the solution, and these ions will get adsorbed on the surface of the metal [19]. In acidic solution, the amine

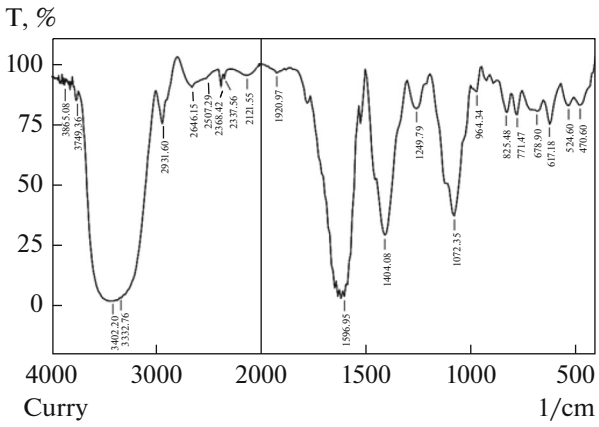

Fig. 9. IR spectrum of solid residue of CLE.

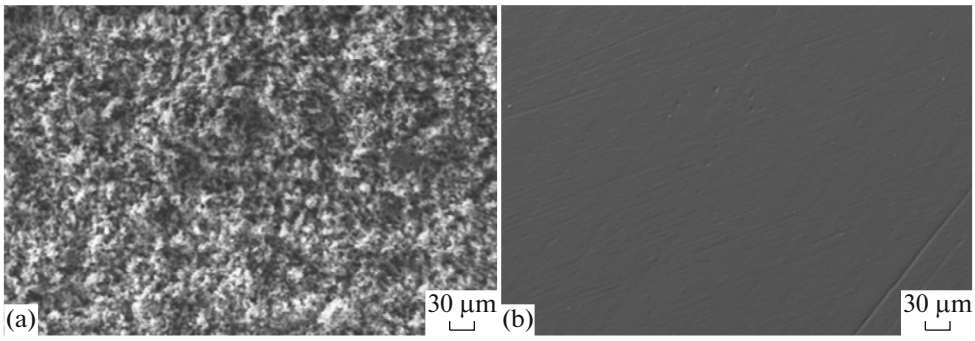

Fig. 10. SEM images of aluminum: (a) in 0.001 M HCl, and (b) in 0.001 M HCl + CLE (0.4 gL^{-1}).

and ether groups of Mahanimbine and the hydroxyl group of Terpene 4-ol present in the CLE can be easily protonated because of their high electron density. The protonated molecules are attracted to the anionic layer formed on the metal surface and get physically adsorbed on it. This will result in the formation of a protective barrier on the surface of the metal. This barrier will prevent further dissolution of the metal and its corrosion. An enhanced corrosion inhibition may be also due to the π electrons of the double bond of constituents of the extract which also acts as high electron rich center [20].

As the inhibitor concentrations increased, the rate of adsorption of the inhibitor molecules on the metal surface also increased. These adsorbed molecules are of a larger size hence they cover the entire metal surface and form a protective film, thereby bringing down both anodic and cathodic reactions under control. So, this film acts as a mixed inhibitor preferentially decreasing the rate of anodic reactions. In these type of adsorption, the force of attraction between the inhibitor and the metal surface may be electrostatic. The unprotonated Mahanimbine, Terpene 4-ol and β-elemene molecules present in the CLE may be chemisorbed on the metal surface on the base of donor–acceptor interactions between π electrons of double bonds in alkene and aromatic rings and vacant *p* orbitals of Al. These chemisorbed molecules diminish the rate of both anodic and cathodic reactions and hence act as a mixed type of the inhibitor.

Table 5. Results of EDX analysis for corrosion inhibition of aluminum using CLE (0.4 gL^{-1}) in hydrochloric acid of pH 3

Medium	Composition, %				
	Al	O	Si	Cl	C
Aluminum in HCl	92.31	7.16	0.37	0.16	–
Aluminum in HCl + CLE (0.4 g L^{-1})	77.02	3.16	0.38	0.04	19.40

Surface Morphology Studies by SEM and EDX Analyses

The SEM images of aluminum in the hydrochloric acid medium of pH 3 in the absence or the presence of the inhibitor are shown in Figs. 10a, 10b, respectively.

The SEM images of aluminum in the hydrochloric acid medium of pH 3 showed the heterogeneous surface, which indicates that the metal undergoes corrosion in the hydrochloric acid medium [19]. The SEM image of aluminum after the addition of the CLE (0.4 gL^{-1}) to the hydrochloric acid medium of pH 3 showed better smoothness of the surface. That is due to the adsorption of constituents of the CLE on the surface of aluminum, which decreases the rate of corrosion.

The interaction of the corrosive with the metal and the adsorption of the inhibitor on its surface was confirmed by the EDX analysis. The results of EDX analysis are tabulated in Table 5. For aluminum immersed in HCl showed % composition for chlorine indicates the interaction of the medium with the metal and for aluminum immersed in HCl containing inhibitor showed % composition for carbon suggests the adsorption of inhibitor onto the metal surface.

CONCLUSIONS

• In a hydrochloric acid medium, the inhibition efficiency of the CLE increases with an increase in its concentration and decreases with an increase in temperature.

• In a hydrochloric acid medium, at lower concentrations of an inhibitor, the CLE functions as the anodic type inhibitor and at higher concentrations of an inhibitor—as a mixed type.

• In a hydrochloric acid medium, the CLE gets adsorbed on the aluminum surface via both physisorption and chemisorption and follows the Langmuir adsorption model.

• In a hydrochloric acid medium, the inhibition efficiency values obtained via PDP and EIS techniques are in good agreement with each other.

• The CLE may be considered to be an effective eco-friendly green inhibitor for the corrosion control of aluminum in the hydrochloric acid medium.

ACKNOWLEDGMENTS

Pushpanjali M. gratefully acknowledges the Department of Chemistry, MIT and Manipal University for providing the laboratory facilities.

REFERENCES

1. Schweitzer, P.A., *Fundamentals of Metallic Corrosion: Atmospheric and Media Corrosion of Metals*, Boca Raton: CRC, 2006, 2nd ed.
2. Ating, E.I., Umoren, S.A., Udousoro, L.I., Ebenso, E.E. and Udoh, A.I., *Green Chem. Lett. Rev.*, 2010, vol. 3, pp. 61–68.
3. El-Etre, A.Y., *Corros. Sci.*, 2003, vol. 45, pp. 2485–2495.
4. Mercier, D. and Barthés-Labrousse, M.G., *Corros. Sci.*, 2009, vol. 51, pp. 339–348.
5. Sanyal, B., *Prog. Org. Coat.*, 1981, vol. 9, pp. 165–236.
6. Bajat, J.B., Mišković-Stanković, V.B., and Kačarević-Popović, Z., *Corros. Sci.*, 2008, vol. 50, pp. 2078–2084.
7. Raja, P.B. and Sethuraman, M.G., *Mater Lett.*, 2008, vol. 62, pp. 113–116.
8. Amitha Rani, B.E. and Basu, B.B.J., *Int. J. Corros.*, 2012, vol. 2012, art ID 380217.
9. Sangeetha, M., Rajendran, S., Muthumegala, S., and Krishnaveni, A., *Zast. Mater.*, 2011, vol. 52, no. 1, pp. 3–19.
10. Parul, S., Javed, A., Neha, B., Honey, J., et al., *Asian J. Pharm. Res.*, 2012, vol. 2, pp. 51–53.
11. Mansfeld, F.B., *Corrosion Mechanisms*, New York: Marcel Dekker, 1987, pp. 165–209.
12. Mansfeld, F., Lin, S., Kim, K., and Shih, H., *Corros. Sci.*, 1987, vol. 27, pp. 997–1000.
13. Mansfeld, F., Lin, S., Kim, K., and Shih, H., *J. Mater. Corros.*, 1988, vol. 39, pp. 487–492.
14. Li, W.H., He, Q., Pei, C.L., and Hou, B.R., *J. Appl. Electrochem.*, 2008, vol. 3, p. 289.
15. *Impedance Spectroscopy: Emphasizing Solid Materials and Systems* Macdonald, J.R., Ed., New York: Wiley, 1987, 2nd ed.
16. Brett, C.M.A., *Corros. Sci.*, 1992, vol. 33, pp. 203–210.
17. Bessone, J.B., Salinas, D.R., Mayer, C., Ebert, M., et al., *Electrochim. Acta*, 1992, vol. 37, p. 2283.
18. Mansfeld, F., *Corrosion-NACE*, Thousands Oaks, CA: Sci. Center, Rockline Int., 1973, vol. 29, no. 10, pp. 397–402. https://doi.org/10.5006/0010-9312-29.10.397.
19. Atinga, E.I., Umoren, S.A., Udousoro, I.I., Ebenso, E.E., et al., *Green Chem. Lett. Rev.*, 2010, vol. 3, p. 61.
20. Oguzie, E.E., Wang, Y. and Li, F.H., *Electrochim. Acta*, 2007, vol. 52, pp. 3950–3957.